European Journal of Radiology 118 (2019) 285–292

Contents lists available at ScienceDirect

European Journal of Radiology

journal homepage: www.elsevier.com/locate/ejrad

Research article

Diagnostic performance of maximum slope: A kinetic parameter obtained from ultrafast dynamic contrast-enhanced magnetic resonance imaging of the breast using k-space weighted image contrast (KWIC)

Akane Ohashi[a], Masako Kataoka[a,*], Shotaro Kanao[b], Mami Iima[a], Katsutoshi Murata[c], Elisabeth Weiland[d], Natsuko Onishi[a], Makiko Kawai[a], Masakazu Toi[e], Kaori Togashi[a]

[a] Department of Diagnostic Imaging and Nuclear Medicine, Kyoto University Graduate School of Medicine, Kyoto, Japan
[b] Kobe City Medical Center General Hospital, Kobe, Hyogo, Japan
[c] Siemens Healthcare K.K., Shinagawa, Tokyo, Japan
[d] Siemens Healthcare GmbH, Erlangen, Germany
[e] Department of Breast Surgery, Kyoto University Graduate School of Medicine, Kyoto, Japan

ARTICLE INFO

Keywords:
Breast cancer
MRI
Ultrafast dynamic contrast-enhanced magnetic resonance imaging
Maximum slope
Delayed washout
Early phase

ABSTRACT

Purpose: To compare the diagnostic performance of the kinetic parameter maximum slope (MS) in breast lesions obtained by ultrafast dynamic contrast-enhanced magnetic resonance imaging (DCE MRI) of the contrast wash-in period with that of the washout index (WI) derived from standard DCE MRI and that of the Breast Imaging Reporting and Data System (BI-RADS) category.

Materials and methods: In total, 138 contrast enhanced lesions (90 malignant, 48 benign) were evaluated. Ultrafast DCE MRI images were acquired using a k-space-weighted image contrast (KWIC), obtained 0–1 min after gadolinium injection (3.75 s/frame; 16 frames) and followed by standard DCE MRI (60 s/frame, 3 frames). MS was calculated for the KWIC time series as percentage relative enhancement per second (%/s). As a semi-quantitative parameter for the standard DCE MRI time series, WI was evaluated using the change in signal intensity between early and delayed phases. The diagnostic performance (malignant/benign differentiation) of MS, WI, and BI-RADS category was compared by ROC analysis using the area under the curve (AUC).

Results: The AUC of MS was as good as that of WI (0.81 vs. 0.79, respectively; P = 0.81), yet inferior to the BI-RADS category (0.81 vs. 0.96, respectively; < 0.001). MS tended to have higher sensitivity (91.1% [82/90]) compared with WI (87.8% [79/90]) with same specificity (62.5% [30/48]).

Conclusions: MS obtained by ultrafast DCE MRI of the breast is a promising kinetic parameter in the differential diagnosis of malignant and benign breast lesions with decreased scanning time.

1. Introduction

Dynamic contrast-enhanced magnetic resonance imaging (DCE MRI) of the breast is regarded as the most sensitive method for detecting breast lesions, although its specificity is relatively low [1]. The American College of Radiology Breast Imaging Reporting and Data System (BI-RADS) suggests that the most important factors in the diagnosis of highly vascularized breast lesions are the delayed-phase kinetic curve and the morphological information of lesions seen on contrast-enhanced breast MRI [1].

Image acquisition with high temporal resolution had been investigated, yet limited to research purposes due to the low spatial resolution as a trade-off [2], making them not feasible in a clinical setting. Thanks to the recent technical advancement, however, bilateral whole-breast image acquisition with high temporal and spatial resolution has become available. These promising techniques include optimized k-space image acquisition, such as the k-space-weighted image contrast (KWIC) sequence [3] and the time-resolve angiography with stochastic trajectories (TWIST) sequence [4] is available as an ultrafast DCE MRI.

Mann et al. recently evaluated the maximum slope (MS) as a novel dynamic parameter for ultrafast DCE acquisition with TWIST sequence,

* Corresponding author at: 54 kawahara-cho Shogoin Sakyo-ku, Kyoto, Japan.
E-mail addresses: amaoh135@gmail.com (A. Ohashi), makok@kuhp.kyoto-u.ac.jp (M. Kataoka), kanaosh@gmail.com (S. Kanao), mamiiima@kuhp.kyoto-u.ac.jp (M. Iima), katsutoshi.murata@siemens-healthineers.com (K. Murata), elisabeth.weiland@siemens-healthineers.com (E. Weiland), natsucom1981@gmail.com (N. Onishi), hiraima.kawai@gmail.com (M. Kawai), toi@kuhp.kyoto-u.ac.jp (M. Toi), ktogashi@kuhp.kyoto-u.ac.jp (K. Togashi).

https://doi.org/10.1016/j.ejrad.2019.06.012
Received 4 July 2018; Received in revised form 14 May 2019; Accepted 11 June 2019
0720-048X/ © 2019 Published by Elsevier B.V.

and showed high accuracy in differentiating between malignant and benign breast lesions compared with delayed-phase kinetic curve analysis [5]. In addition, Goto et al. evaluated the diagnostic performance of breast ultrafast MRI using MS in combination with BI-RADS, showing its usefulness in diagnosing NME (non mass enhancement) lesions [6]. However, there is limited evidence on direct comparison of diagnostic performance between MS and standard BI-RADS based diagnosis.

The purpose of this study was to examine the diagnostic performance of MS obtained by ultrafast DCE MRI using the KWIC sequence in breast lesions. The diagnostic performance of MS was then compared with that of 1) the washout index (WI), a kinetic parameter which is a quantitative value of delayed washout obtained from the standard DCE sequence, and 2) the overall assessment of the BI-RADS category.

2. Material and methods

2.1. Patients

This study was approved by our institutional review board, with retrospective design. Because KWIC prototype sequence was obtained as a part of the hybrid protocol with standard DCE MRI and the scanning time was completely the same as our standard clinical protocol, the need for informed consent was waived. The study population comprised 205 patients with suspected breast cancer had undergone contrast-enhanced breast MRI that included ultrafast KWIC acquisitions during the inflow phase of the DCE MRI from June 2013 to April 2014. In cases of multiple lesions in one breast, the most enhanced lesions on KWIC images were included in the analysis. The inclusion criteria was the presence of histopathologically diagnosed lesions or lesions which were confirmed as benign and the absence of tumor growth for more than 24 months follow-up by ultrasound or MRI. The exclusion criteria was for those who had a current or past neoadjuvant endocrine or chemotherapy (n = 45), no detectable enhancing lesion (n = 23), failed image analysis because of incomplete image transfer (n = 4), and less than 24 months follow-up period for benign lesions (n = 14). In total, 119 patients (mean age, 56.0 years old; age range, 20–87 years old) with 138 lesions (90 malignant, 48 benign) were included in this analysis. Malignant lesions were histopathologically diagnosed through biopsy. Benign lesions were diagnosed through biopsy, otherwise, the absence of tumor growth during their follow-up period for at least 24 months (23/48 lesions, average follow up period was 50.6 months) by ultrasonography or MRI. Average interval between MR study and tissue sampling were 12.2 days (1–65 days) for benign lesions and 7.4 days (0–58 days) for malignant lesions. All pathologic results were defined according to the World Health Organization classification of breast tumors [7].

2.2. Standard MRI acquisition

All breast MRI studies were performed with a 3 T scanner (MAGNETOM Trio, A Tim System; Siemens Healthcare GmbH, Erlangen, Germany) with a 16-channel dedicated bilateral breast coil. T2-weighted, T1-weighted, diffusion-weighted, and fat-suppressed T1-weighted DCE images were obtained as part of the standard DCE MRI examination. The MRI parameters were as follows. T2-weighted images: whole breast, axial orientation; repetition time/echo time (TR/TE), 5500/77 ms; and thickness, 3.0 mm. T1-weighted images: whole breast, axial orientation; 3D-gradient echo; TR/TE, 4.8/2.5 ms; and thickness, 1.5 mm. Diffusion-weighted images: whole breast, axial orientation; single-shot echo-planar imaging; TR/TE, 7000/62 ms; field of view (FOV), 330 × 185.4 mm^2; matrix, 162 × 92; thickness, 3.0 mm; number of excitations, 3; 48 slices; and b value, 0 and 1000s/mm^2. Fat-suppressed T1-weighted DCE images: one pre-contrast and two post-contrast (1–2 and 5–6 min after gadolinium injection) whole-breast axial scans at high temporal resolution with contrast enhancement for 1 min with the following parameters: 3D-volumetric interpolated breath-hold examination (VIBE); TR/TE, 3.9/1.5 ms; flip angle (FA), 15; FOV, 330 × 330 mm^2; matrix, 384 × 384; thickness, 1.0 mm; post-contrast (2–5 min after gadolinium injection) whole-breast coronal scan at high spatial resolution (3D-VIBE; TR/TE, 4.2/1.7 ms; FA, 15; FOV, 330 × 330 mm; matrix, 512 × 512; and thickness, 0.8 mm). The infused gadolinium contrast materials were gadoteridol (ProHance; Eisai Inc., Tokyo, Japan) at a dose of 0.2 mmol/kg, power-injected at a speed of 2.0 ml/s and flushed with 20 ml of saline at the same speed of 2.0 ml/s.

2.3. KWIC sequence

The KWIC prototype sequence was obtained 0 to 1 min after gadolinium injection, before the early postcontrast scan using 3D-VIBE. The parameters are as follows: TR/TE, 3.6/1.7 ms; FA, 15; FOV, 330 × 330 mm^2; matrix, 352 × 352; slice thickness, 2.5 mm; temporal resolution, 3.75 s/frame (16 frames with 60 slices, total of 960 images). The KWIC sequence applies a radial acquisition of the k-space together with view sharing to provide high temporal resolution [8]. The KWIC acquisition parameters were adopted and modified from the study by Mann et al. [5] using the TWIST sequence, which applies view sharing in combination with a Cartesian k-space sampling with a spatial resolution of 0.9 × 0.9 × 2.5 mm and a temporal resolution of 4.3 s/frame.

Schematic drawing of the interleaving of the KWIC protocol with the standard dynamic VIBE protocols is shown in Fig. 1. The scan parameters of the KWIC and standard dynamic VIBE protocols are summarized in Table 1.

2.4. Image analysis

The characteristics of the contrast inflow of the KWIC phases were evaluated using dedicated software (TWIST Breast Viewer, prototype software; Siemens Healthcare GmbH, Erlangen, Germany). MS was calculated as the difference quotient from the change of relative enhancement among three time points, divided by the time (Fig. 2). To

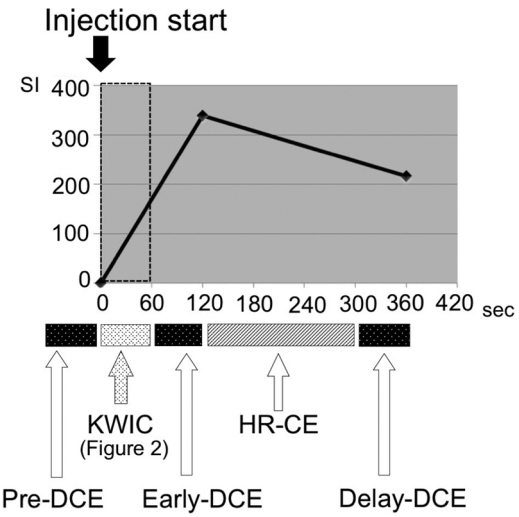

Fig. 1. Schematic drawing of the breast magnetic resonance imaging protocol with k-space-weighted image contrast (KWIC) sequence.
Our standard dynamic protocol consists of one pre-contrast and two post-contrast. 3D-volumetric interpolated breath-hold examination measurements with a 1-min acquisition duration and high-resolution contrast enhancement between the two post-contrast measurements. In this study, we inserted the KWIC sequence directly after contrast injection into our standard dynamic protocol. A typical time–intensity curve for a malignant lesion is shown.
Details of KWIC is in Fig. 2. Abbreviations: DCE: dynamic contrast enhance; HR-CE: high resolution contrast enhance; SI: signal intensity.

Table 1
Scan parameters of the breast MRI protocol.

Protocol	KWIC	Dynamic (VIBE)
Base sequence	3D FLASH	3D FLASH
TR/TE (ms)	3.6/ 1.7	3.9/ 1.5
Flip Angle (degree)	15	15
Number of time points	16 (16 post) (3.75 sec/ frame)	3 (1 pre, 2 post) (60 sec/ frame)
Slice thickness (mm)	2.5	1
FOV (mm)	330 × 330	330 × 330
Resolution (mm)	0.94 × 0.94 (60 slices)	0.86 × 0.86 (144 slices)
Matrix	352 × 352	384 × 384
Fat-suppression	SPAIR	SPAIR
iPAT	NA	3

These protocols use different temporal resolutions and slice thicknesses, but the spatial resolution of both protocols is in accordance with the EUSOBI guideline (in-plane resolution of 1 mm, slice thickness of ≤ 2.5 mm).
KWIC: k-space weighted imaging contrast, VIBE: 3D-volumetric interpolated breath-hold examination, FLASH: fast low-angle shot, TR/TE: repetition time/ echo time, FOV: field of view, SPAIR: spectral attenuated inversion recovery, iPAT: integrated parallel acquisition techniques, NA: not applicable.

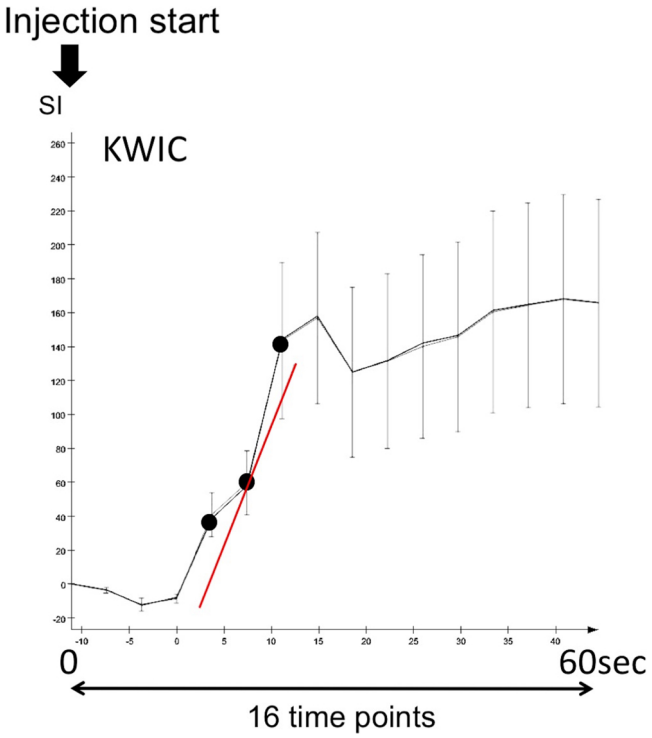

Fig. 2. Calculation of maximum slope from k-space-weighted image contrast (KWIC).
Our KWIC sequence uses 16 time points in the first 60 s after injection of the contrast agent. This graph shows the signal intensity change in the region of interest at the most strongly enhancing area of the lesion. The slope is calculated with dedicated software (TWIST breast viewer) using three adjacent time points of the graph, and the steepest (red line) slope is selected as the maximum slope. It is presented in units of percentage relative enhancement per second (%/s).

quantify the value of the highest MS, color coded MS maps were used to identify the hotspot of the lesion and placing as many non-overlapping 3 × 3 mm circular ROIs as possible inside it manually using AQ net viewer (TERA recon). Two radiologists specializing in breast imaging for 18 and 5 years, respectively (M.K. and A.O.), quantified the MS ROIs to evaluate intra-class correlation coefficient (ICC) two years after the BI-RADS reporting archives. As kinetic information obtained from standard DCE sequence, we evaluated the washout index (WI) from the conventional DCE MRI in the ROI with the lowest value with the same voxel size as MS. WI was defined as follows: WI = (signal intensity [SI] delay − SI early) / SI pre × 100%. Both curves were extracted independently. Representative cases with a color-coded map of MS and a time–intensity curve were shown in Figs. 3 and 4.

2.5. BI-RADS category evaluations

Morphological evaluation was performed using BI-RADS MRI descriptors according to the fifth edition [1]. Lesions considered probably benign were categorized as BI-RADS 2 (likelihood of malignancy: LOM 0%) or 3 (LOM < 2%). Lesions suspicious for malignancy were categorized as BI-RADS 4 (LOM 2–95%), and highly suggestive of malignancy were categorized as BI-RADS 5 (LOM 95% <).

The BI-RADS category of each lesion was stored on the MRI reporting archives in our institution as described by two radiologists who had been specialized in breast imaging for 18 and 17 years, respectively (M.K. and S.K.) at the time of diagnosis.

In the original reports, 19 lesions were described as category 6 (known malignancy), and their BI-RADS categories and probability of malignancy were not based on imaging. The MRI scans of these 19 lesions were re-assessed based on BI-RADS MRI by a radiologist blinded to the final pathology and mixed with other lesions from category 5 (n = 11), 4 (n = 8), 3 (n = 1), and 2 (n = 1) randomly selected from the remaining population.

2.6. Statistical analysis

Receiver operating characteristic (ROC) analysis of the discriminating diagnostic performance of MS, WI and BI-RADS category for each lesion was performed using histopathology or follow-up as the reference standard. The diagnostic performance of MS was compared with that of WI and BI-RADS category using ROC analysis to differentiate benign from malignant breast lesions, followed by subgroup analysis for mass and non-mass enhancement (NME). Because of the small number of cases, focus was included in NME for analysis. Numerical value of BI-RADS Category was used directly for ROC analysis [9]. The comparison of two areas under the ROC curve (AUCs) was conducted based on the DeLong test.

The optimal cut-off points for WI in discriminating malignant and benign lesions in this study population were determined based on the maximum value of the sum of the sensitivity and specificity (Youden index) for MS and WI. False-positive and false-negative lesions according to MS and WI were further analyzed with respect to their association with the pathological diagnosis.

The agreements of MS values by two radiologists were evaluated using intra-class correlation coefficients (ICC). ICC was defined as: ≤ 0.40, poor agreement; 0.40–0.59, fair agreement; 0.60–0.74, good agreement; 0.75–1.00, excellent agreement [10].

All *P*-values were two-sided, and *P*-values of ≤0.05 were considered statistically significant. Statistical analyses were performed with EZR (Saitama Medical Center, Jichi Medical University; http://www.jichi.ac.jp/saitama-sct/SaitamaHP.files/statmedEN.html), which is a graphical user interface for R, version 2.13.0 (The R Foundation for Statistical Computing, Vienna, Austria). More precisely, it is a modified version of R commander (version 1.6–3) designed to add statistical functions frequently used in biostatistics. ICC statistics and cut-off points for MS and WI were calculated using STATA version 13 (STATA Corp., Texas, USA).

3. Results

3.1. Lesions

In total, 138 enhancing lesions (105 masses, 29 non-mass enhancements, 4 foci) in 119 patients were selected for this study. Among

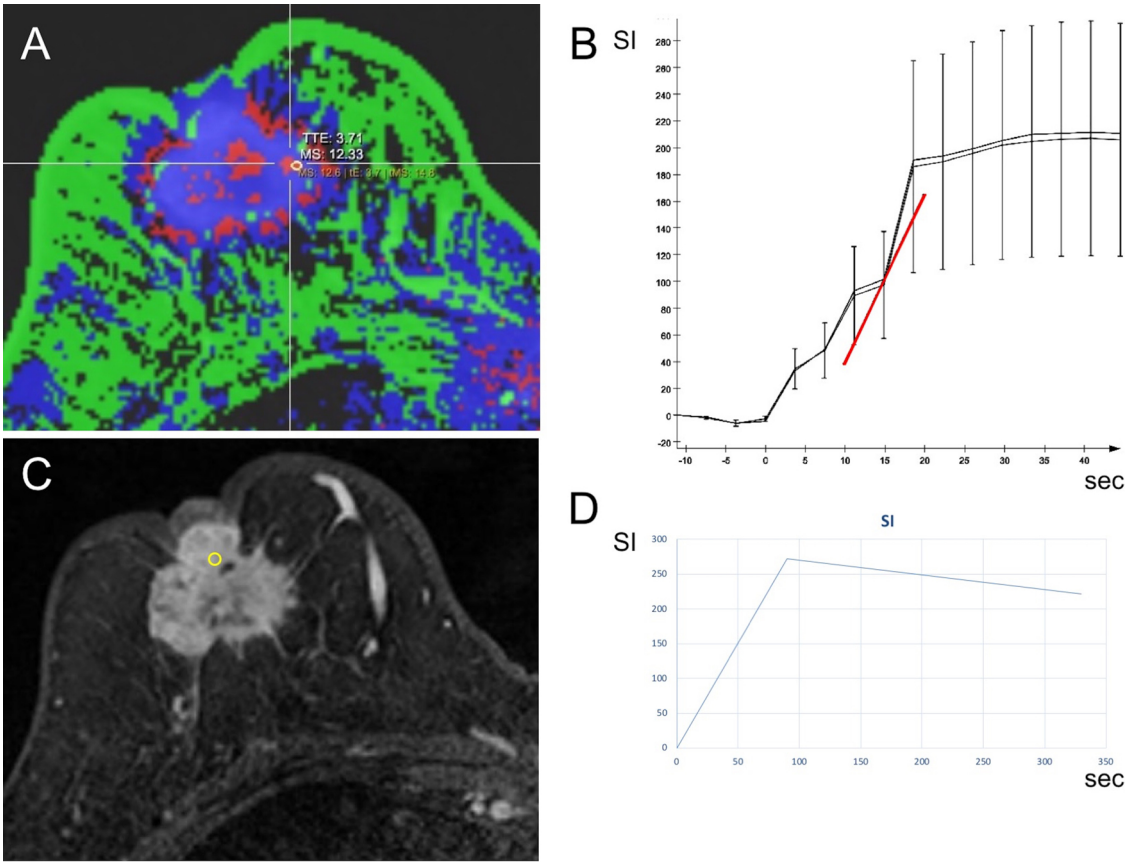

Fig. 3. Representative case of malignant lesion (invasive carcinoma of no special type).
(A) Color map of maximum slope (MS). MS values of > 9.76%/s were colored red, suggesting a high probability of malignancy. (B) Time–intensity curve of k-space-weighted image contrast. The MS (12.3%/s) was high, indicating malignancy. (C) The same lesion on early phase of standard dynamic contrast-enhanced imaging. (D) Time–intensity curve of standard dynamic protocol. This lesion showed a delayed washout. Malignancy was suggested by both MS value and standard dynamic contrast enhanced imaging. SI: signal intensity.

them, 90 lesions were malignant (average size: 26.2 mm) and 48 lesions were benign (average size: 13.9 mm). Average size and SD per BI-RADS category shown in Table 2. Average size of category 2 and 3 lesions were smaller than category 4 and 5. All lesions were visible in KWIC images and standard DCE MRI. The detailed pathological diagnoses of these lesions are presented in Table 3.

3.2. BI-RADS evaluation

BI-RADS categories and each frequency of malignancy is shown in Table 4A. The frequency of malignancy was 0% in category 2 and 3, 53% in category 4, 100% in category 5, among total lesions. The trend was same in both mass and NME.

Suspicious findings from each BI-RADS categories are summarized in Table 4B. The irregular shape, not-circumscribed margin, and rim-enhancement in masses, and segmental distribution in NMEs showed higher probability of malignancy.

3.3. Kinetic parameters on DCE MRI

Intra-class correlation coefficients (ICC) of two readers was 0.98 (95% confidence interval; 0.97-0.99) indicating almost perfect inter reader agreement. Hence, MS between two radiologists were averaged for each lesion.

The average MS was 25.1%/s (standard deviation: SD, 11.4%/s) for malignant lesions and 12.4%/s (SD, 11.0%/s) for benign lesions (Table 5). Box plots of MS and WI are shown in Fig. 5. The average MS of malignant lesions were higher than that of benign lesions, and the average WI of malignant lesions were lower than that of benign lesions; however, the overlap of values were present between malignant and benign lesions. On ROC analysis, AUC of MS was similar to that of WI with marginal significance (0.81 vs. 0.79, respectively; $P = 0.81$). The AUC of MS was significantly lower than that of the BI-RADS category (0.81 vs. 0.96, respectively; $P < 0.001$) (Table 6, Fig. 6).

Subgroup analysis was performed for mass and NME (including focus). In mass, the AUC of MS was comparable to WI (0.76 vs. 0.79, respectively; $P = 0.71$), and the AUC of MS was significantly lower than that of the BI-RADS category (0.76 vs. 0.97, respectively; $P < 0.001$). In the NME, the AUC of MS was as good as that of WI (0.72 vs. 0.69, respectively; $P = 0.79$), and the AUC of MS tended to be lower than that of the BI-RADS category, without statistically significant difference (0.72 vs. 0.85, respectively; $P = 0.22$) (Table 6). Representative figures for mass and NME were presented in Figs. 3 and 4.

3.4. Cut-off values of MS and WI

The optimal cut-off points determined by the Youden index were > 9.76% /s for MS and < −25% for WI. Based on these cut off points, giving a sensitivity, specificity of 91.1% [82/90] and 62.5% [30/48] for MS, 87.8% [79/90] and 62.5% [30/48] for WI (Table 7). On the other hand, PPV and NPV were almost comparable (PPV; 82.0% [82/100] and NPV; 78.9% [30/38] for MS, PPV; 81.4% [79/97] and NPV; 73.2% [30/41] for WI).

Lesions with a discrepant diagnosis (false-positive and false-negative lesions based on MS and WI) were further analyzed with respect to their association with the pathological diagnosis (Table 8). The number

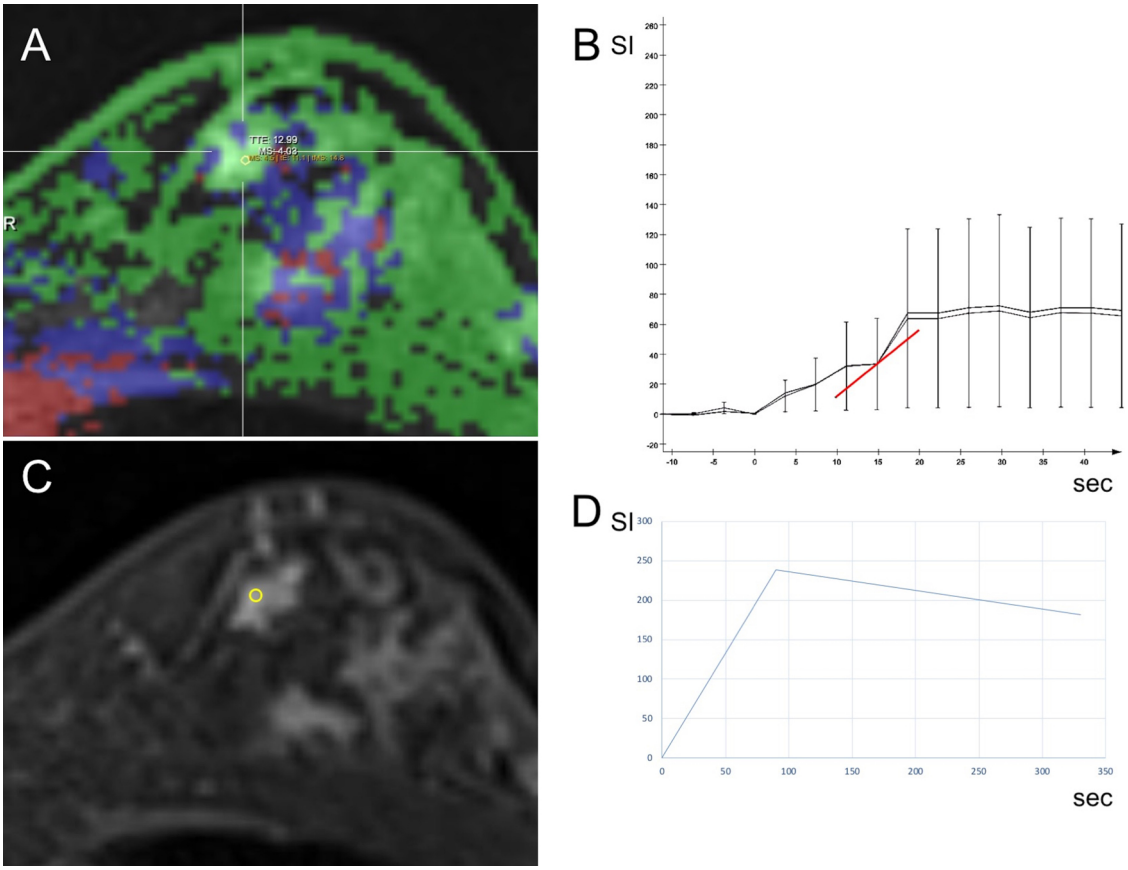

Fig. 4. Representative case of benign lesion (fibrocystic change).
(A) Color-coded map of the maximum slope (MS). MS values of < 9.76%/s is colored blue and green, indicating benign lesions. (B) Time–intensity curve of the ROI corresponding to the lesion. The MS value was relatively low (4.0%/s.). (C) Early phase of standard dynamic contrast-enhanced imaging. (D) Time intensity curve of standard dynamic protocol. This lesion showed delayed washout and was categorized as malignant based on standard dynamic contrast-enhanced imaging.

Table 2
Average size and SD per BI-RADS category.

	Total		Malignant		Benign	
Category	n	Average ± SD (cm)	n	Average ± SD (cm)	n	Average ± SD (cm)
2	11	13.9 ± 4.9	0	–	11	13.9 ± 4.9
3	19	15.7 ± 16.7	0	–	19	15.7 ± 16.7
4	38	18.8 ± 19.2	20	25 ± 24.4	18	12.1 ± 7
5	70	26.6 ± 15.7	70	26.6 ± 15.7	0	–
Total	138	21.9 ± 16.9	90	26.2 ± 17.8	48	13.9 ± 11.3

SD: Standard Deviation, BI-RADS: Breast Imaging Reporting and Data System.

Table 3
Pathological diagnosis of the lesions.

Lesion type	n	Lesion type	n
Malignant	90	Benign	48
NST	71	FCC	23
DCIS	9	FA	15
ILC	4	IDP	3
IMPC	2	Inflammation	2
Mucinous carcinoma	2	FEA	1
ICPC	1	Other	4
Lymphoma	1		

NST: invasive carcinoma of no special type, DCIS: ductal carcinoma in situ, ILC: invasive lobular carcinoma, IMPC: invasive micropapillary carcinoma, ICPC: intra cystic papillary carcinoma, FCC: fibrocystic change, FA: fibroadenoma, IDP: intra ductal papilloma, FEA: flat epithelial atypia.

of false-negative cases were the almost same for MS and WI (n = 8/9). Fibrocystic change in false positive cases were 5/8 (62.5%) with WI and 3/8 (37.5%) with MS. It might indicate that MS tends to correctly diagnose fibrocystic change as benign lesions based on low vascularity, fibrocystic change tends to have milder slope on the ultrafast DCE MRI. The MS map and corresponding time–intensity curve of the WI-based false-positive case (fibrocystic change) was shown in Fig. 4. However, some fibroadenomas were falsely diagnosed as malignant lesions due to their high vascularity.

4. Discussion

In this study, we compared the diagnostic accuracy of two kinetic parameters: MS and WI. MS tended to provide similar diagnostic

Table 4A
Frequency of malignant lesion by BI-RADS category.

	Total			Mass			NME			Focus		
Category	Total (n)	Malignant (n)	%	Total (n)	Malignant (n)	%	Total (n)	Malignant (n)	%	Total (n)	Malignant (n)	%
2	11	0	0	9	0	0	2	0	0	0	0	0
3	19	0	0	8	0	0	8	0	0	3	0	0
4	38	20	53	21	12	55	16	8	50	1	0	0
5	70	70	100	67	67	100	3	3	100	0	0	0
Total	138	90	64	105	79	71	29	11	38	4	0	0

Table 4B
Frequency of Malignant lesions by BI-RADS morphology.

		Mass			NME		
		Total (n)	Malignant (n)	%	Total (n)	Malignant (n)	%
Mass	Irregular shape	61	56	92			
	Not-circumscribed margin	78	74	95			
	Rim enhancement	61	60	98			
NME	Segmental/ linear distribution				11	9	82
	Heterogeneous enhancement				20	9	45
	Clumped				10	2	20
	Clustered ring				6	4	67

%: Frequency of malignant lesion.
BI-RADS: Breast Imaging Reporting and Data System, NME: non-mass enhancement.

Table 5
Summary of Maximum Slope (MS) and Washout Index (WI).

		MS (%/s)	WI (%)
	n	Average ± SD	Average ± SD
Total	138	20.7 ± 12.7	−55.5 ± 54.1
Malignant vs. Benign			
Malignant	90	25.1 ± 11.4	−73.9 ± 48.8
Benign	48	12.4 ± 11.0	−20.9 ± 46.4
Mass vs. NME			
Mass	105	23.9 ± 12.4	−65.1 ± 54.2
NME	33	10.6 ± 7.6	−25.0 ± 41.4

SD: standard deviation, NME: Non-mass enhancement.
Focus is included in NME.

performance for malignant breast lesions as WI (Fig. 6). In a recent study of ultrafast dynamic evaluation, the accuracy of MS was significantly higher than that of conventional kinetic analysis to distinguish malignant and benign lesions [5,11]. Other recent study using ultrafast imaging showed comparable diagnostic performance of initial enhancement ratio (the ratio of pre to early enhancement) or time to enhance (TTE) to that of standard kinetic assessment, suggesting the usefulness of early initial enhancement analysis [12,13]. These reports and our results suggest that ultrafast DCE MRI may be an alternative to conventional DCE MRI.

Our comparison of MS and WI indicated that MS compensated for the weakness of the low diagnostic specificity of standard DCE MRI. Some lesions with FCC may show a washout kinetics pattern and mimic malignancy [14,15]. In the present study, MS tends to correctly diagnose fibrocystic changes as benign lesions, which often shows a malignant washout pattern and is judged as malignant when using WI. If MS and WI show discrepant results, careful evaluation and consideration of the underlying pathology may help to refine the diagnosis.

The diagnostic accuracy of MS and WI were inferior to the overall assessment using the BI-RADS category including morphological information (Fig. 6). Our findings indicate that morphological information is still important in the diagnosis of breast lesions. The presence of benign hypervascular masses such as papillomas or fibroadenomas may result in a false-positive diagnosis based on kinetic information, even with MS, as in the present study (Table 8). However, the morphological

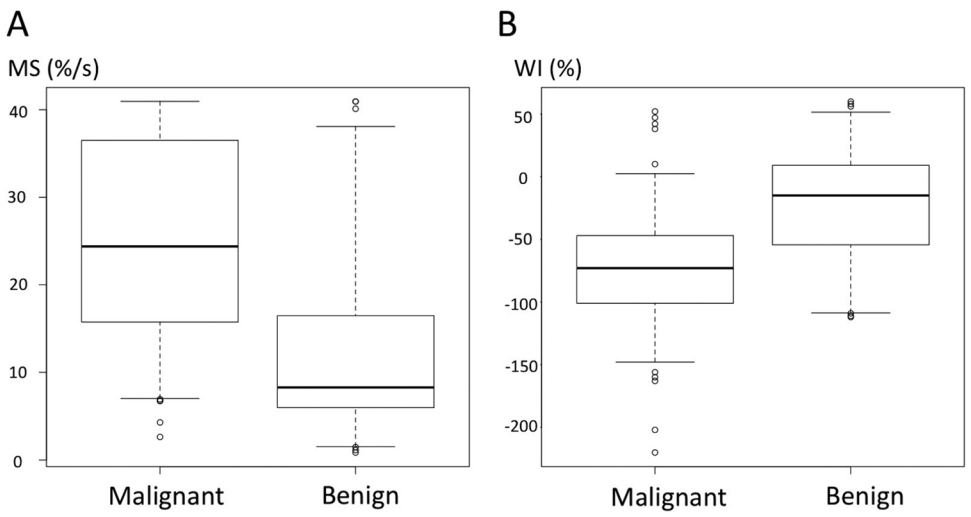

Fig. 5. Box plot of the Maximum Slope (MS) and Washout Index (WI).
(A) Box plot of the Maximum Slope (MS) shows that malignant lesions had a higher value than benign lesions. (B) Box plots of the Washout Index (WI) shows that most of the malignant lesions demonstrated wash out on delayed phase. WI is defined as difference between signal intensity (SI) on delayed phase and SI on early phase of dynamic contrast enhanced image. Negative value means decrease of SI in the delayed phase.

Table 6
Area under the ROC Curves (AUC) of Maximum Slope (MS), Washout Index (WI), and BI-RADS Category.

		AUC	*p*-value*
Total (n = 138)	MS	0.81 [0.72-0.89]	
	WI	0.79 [0.71-0.88]	0.81
	BI-RADS	0.96 [0.94-0.98]	< 0.001
Mass (n = 105)	MS	0.76 [0.64-0.88]	
	WI	0.79 [0.67-0.90]	0.71
	BI-RADS	0.97 [0.95-0.99]	< 0.001
NME (n = 33)	MS	0.72 [0.51-0.93]	
	WI	0.69 [0.49-0.88]	0.79
	BI-RADS	0.85 [0.76-0.95]	0.22

All lesions are divided into masses (n = 105; 26 benign, 79 malignant) and NMEs (n = 33; 22 benign, 11 malignant). Four foci (all benign) are included in NME.
*P value was calculated by comparing AUC between MS and WI (or BI-RADS Category) using DeLong test.
Data in brackets are 95% confidence intervals.
ROC curve: receiver operating characteristic curve, AUC: area under curve, BI-RADS: Breast Imaging Reporting and Data System, NME: non-mass enhancement.

Table 7
Diagnostic performance of Maximum Slope (MS) and Washout Index (WI).

	Sensitivity (%)	Specificity (%)	PPV (%)	NPV (%)
MS	91.1(82/90) [83.2-96.1]	62.5 (30/48) [47.4-76.0]	82.0 (82/100) [73.1-89.0]	78.9 (30/38) [62.7-90.4]
WI	87.8 (79/90) [79.2-93.7]	62.5 (30/48) [47.4-76.0]	81.4 (79/97) [72.3-88.6]	73.2 (30/41) [57.1-85.8]

Cut off values: MS, 9.76%/s; WI, −25.0%.
Data in parenthesis are raw data; data in brackets are 95% confidence intervals.
PPV = positive predictive value, NPV = negative predictive value.

Table 8
List of false-positive and false-negative lesions based on Maximum Slope (MS) and/or Washout Index (WI).

Discrepancy	Lesion Type	Total	Mass	NME
False Positive based on WI only	FCC	5	1	4
	IDP	2	1	1
	FEA	1	0	1
False Positive based on MS only	FCC	3	1	2
	FA	5	5	0
False Positive based on MS and WI	FCC	4	3	1
	FA	4	4	0
	IDP	1	1	0
	Granulomatous mastitis	1	1	0
False Negative based on MS only	NST	4	4	0
	DCIS	2	0	2
False Negative based on WI only	NST	6	5	1
	ILC	1	1	0
False Negative based on MS and WI	DCIS	1	1	0
	Mucinous Carcinoma	1	1	0

Cut off values: MS, 9.76%/s; WI, −25.0%.
Abbreviations of the pathological diagnosis are the same as in Table 3.

characteristics of these lesions (shape and margins) helped to avoid such a misclassification (Table 4B).

Based on these results, MS cannot replace the overall BI-RADS category by itself. However, among kinetic parameters, MS performed similarly to WI in predicting malignancy. Thus, adding MS into the morphological information of the BI-RADS category may provide similar diagnostic performance as the overall BI-RADS category with washout kinetics. A recent study showed improved diagnostic performance when MS was combined with morphological information [6,11].

Recently, many studies have established the use of contrast enhanced breast MRI for screening modality [16]. Also abbreviated breast MRI is a shortened version of standard breast MRI protocol for screening MRI, which was first reported by Kuhl et al. [17]. And the combination of both methods allows shortened scan time of breast MRI for screening. Recent studies demonstrated that adding ultrafast to abbreviated fast imaging improves diagnostic performance of benign lesions compared to full protocol imaging [18]. Jan et al. compared ultrafast protocol to full MRI protocol for breast screening, and it showed improving specificity (0.76 full diagnostic vs. 0.82 ultrafast, p = 0.50) without decreasing sensitivity [19]. Mehmet et al. used artificial intelligence classification with ultrafast DCE MRI, T2WI and DWI (ADC), combining these imaging methods with patients information (age and BRCA status). This paper indicates that using ultrafast imaging alone is sufficient, and even higher diagnostic ability can be obtained combined with other information [20]. Our results are in line with these reports. If morphological information can be obtained during an early phase of dynamic image, combination of morphological information with MS will be a promising strategy for reducing scan time on breast MRI. This, of course, should be verified in future studies.

Although we use MS for a kinetic parameter in this study to analyze ultrafast DCE MRI, several parameters have been investigated. Abe

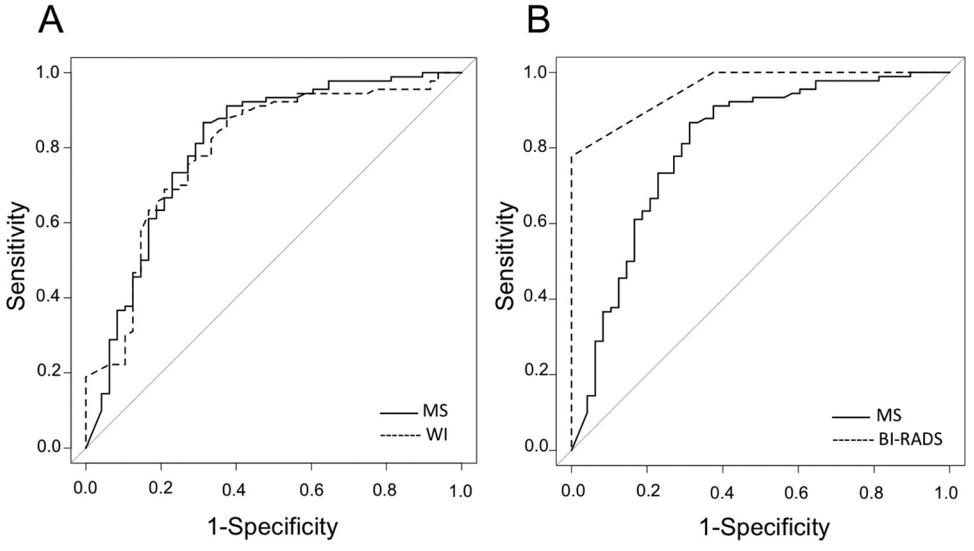

Fig. 6. Receiver operating characteristic curve (ROC) analysis of Maximum Slope (MS), Washout Index (WI), and BI-RADS category in all lesions (n = 138; 48 benign, 90 malignant). (A) Receiver operating characteristic curve of the maximum slope (MS) and washout index (WI). (B) Receiver operating characteristic curve of the MS and Breast Imaging Reporting and Data System (BI-RADS) category. The area under the curve of MS was similar to that of WI (0.81 vs. 0.79, respectively; $p = 0.81$), and the area under the curve of MS was significantly lower than that of the BI-RADS category (0.81 vs. 0.96, respectively; $p < 0.001$).

et al. used enhancement rate or increasing rate of signal intensity [12], and Mori et al. used an empirical mathematical model (EMM) (a model fitting) [21] for differentiating benign from malignant lesions. MS and other kinetic features with quantitative nature can be used for computer-based analysis [11]. These new kinetic parameters may be a candidate for new biomarkers.

A subgroup analysis for mass and NME were performed because an early study by Gutierrez et al. [22] suggested that the diagnostic ability of mass and NME were different in terms of their BI-RADS characteristics. In our subgroup analysis, the ROC ratio of MS and WI in mass showed similar trends as in all lesions (Table 6). However, this was not applicable to NME because of the small number of cases in the present study.

Our study has several limitations. First, this is a preliminary analysis with a relatively small sample size, therefore underpowered to conclude equality of these parameters in non-inferiority study. The current results should be verified in a larger study. Second, AUC of BI-RADS category is very high. There are two possible reasons. BI-RADS category is reported in the clinical site where clinical and non-MRI information may be available for radiologists to increase diagnostic accuracy. Another reason is that lesion size may help to diagnose larger malignant lesions from smaller benign lesions. Third, assessment of BI-RADS is unevenly categorized into the likelihood of malignancy. It might not be ideal to compare these ordinal variables with continuous variables like MS [9]. We would like to consider a better way in the future. Finally, the temporal information obtained from KWIC may not have been accurate because KWIC has information in common with adjacent time frames in image reconstruction. The accuracy of MS might be improved by continued progress and improvements in imaging methods. For example, compressed sensing, a new high-speed MRI acquisition technique that provides more accurate temporal information, may overcome this technical shortcoming.

5. Conclusion

MS obtained by ultrafast DCE MRI of the breast using KWIC is a promising kinetic parameter in the differential diagnosis of malignant and benign breast lesions. The results indicate the potential of DCE MRI protocol with decreased scanning time compared to the conventional standard DCE MRI in line with other previous studies [5,6,11–13]. Patterns of false positive and false negative were slightly different between MS and WI based diagnosis. The diagnostic performance of MS, however, were inferior to that of the BI-RADS category, suggesting contribution of morphologic information in diagnosing breast lesions.

Declaration of Competing Interest

Katsutoshi Murata, MSc is employed by Siemens Healthcare K.K., Japan.

Elisabeth Weiland, PhD is employed by Siemens Healthcare GmbH, Germany.

All the other authors below declare no conflict of interest.

Akane Ohashi, MD, Masako Kataoka, MD, PhD, Shotaro Kanao, MD, PhD, Mami Iima, MD, PhD, Natsuko Onishi, MD, PhD, Makiko Kawai, MD, Masakazu Toi, MD, PhD, Kaori Togashi, MD, PhD

Funding

This work was supported by a Grant-in-Aid for Scientific Research “Evaluation of Wash in Phase in Breast MRI using Ultrafast Imaging” (Grant Number JP15K09922).

Role of the funding source

The funders had no role in study design, data collection and analysis, decision to publish, or preparation of the manuscript.

Acknowledgements

We thank Dr. Yoshiki Mikami and Dr. Tatsuki R. Kataoka for support with the pathological diagnosis. The pathological information were obtained at the Department of Diagnostic Pathology, Kyoto University Graduate School of Medicine. Also we thank Dr. Ayami Ohno Kishimoto, Dr. Maya Honda, Dr. Rie Ota, Department of Diagnostic Imaging and Nuclear Medicine, Kyoto University Graduate School of Medicine, for their support with manuscript editing.

References

[1] E.A. Morris, C.E. Comstock, C.H. Lee, et al., ACR BI-RADS® Magnetic ResonanceImaging. In: ACR BI-RADS® Atlas, Breast Imaging Reporting and DataSystem, American College of Radiology, Reston, VA, 2013.
[2] C.K. Kuhl, H.H. Schild, N. Morakkabati, Dynamic bilateral contrast-enhanced MR imaging of the breast: trade-off between spatial and temporal resolution, Radiology 236 (3) (2005) 789–800.
[3] H.K. Song, L. Dougherty, Dynamic MRI with projection reconstruction and KWIC processing for simultaneous high spatial and temporal resolution, Magn. Reson. Med. 52 (4) (2004) 815–824.
[4] Y. Le, H. Kipfer, S. Majidi, S. Holz, B. Dale, C. Geppert, R. Kroeker, C. Lin, Application of time-resolved angiography with stochastic trajectories (TWIST)-Dixon in dynamic contrast-enhanced (DCE) breast MRI, J. Magn. Reson. Imaging 38 (5) (2013) 1033–1042.
[5] R.M. Mann, R.D. Mus, J. van Zelst, C. Geppert, N. Karssemeijer, B. Platel, A novel approach to contrast-enhanced breast magnetic resonance imaging for screening: high-resolution ultrafast dynamic imaging, Invest. Radiol. 49 (9) (2014) 579–585.
[6] M. Goto, K. Sakai, H. Yokota, M. Kiba, M. Yoshida, H. Imai, E. Weiland, I. Yokota, K. Yamada, Diagnostic performance of initial enhancement analysis using ultra-fast dynamic contrast-enhanced MRI for breast lesions, Eur. Radiol. (2018).
[7] W. Böcker, WHO classification of breast tumors and tumors of the female genital organs: pathology and genetics, Verh. Ges. Pathol. 86 (2002) 116–119.
[8] H.K. Song, L. Dougherty, k-space weighted image contrast (KWIC) for contrast manipulation in projection reconstruction MRI, Magn. Reson. Med. 44 (6) (2000) 825–832.
[9] N.A. Obuchowski, Receiver operating characteristic curves and their use in radiology, Radiology 229 (1) (2003) 3–8.
[10] D.V. Cicchetti, Guidelines, criteria, and rules of thumb for evaluating normed and standardized assessment instruments in psychology, Psychol. Assess. 6 (4) (1994) 284–290.
[11] B. Platel, R. Mus, T. Welte, N. Karssemeijer, R. Mann, Automated characterization of breast lesions imaged with an ultrafast DCE-MR protocol, IEEE Trans. Med. Imaging 33 (2) (2014) 225–232.
[12] H. Abe, N. Mori, K. Tsuchiya, D.V. Schacht, F.D. Pineda, Y. Jiang, G.S. Karczmar, Kinetic analysis of benign and malignant breast lesions with ultrafast dynamic contrast-enhanced MRI: comparison with standard kinetic assessment, AJR Am. J. Roentgenol. 207 (5) (2016) 1159–1166.
[13] R.D. Mus, C. Borelli, P. Bult, E. Weiland, N. Karssemeijer, J.O. Barentsz, A. Gubern-Mérida, B. Platel, R.M. Mann, Time to enhancement derived from ultrafast breast MRI as a novel parameter to discriminate benign from malignant breast lesions, Eur. J. Radiol. 89 (2017) 90–96.
[14] J.H. Chen, O. Nalcioglu, M.Y. Su, Fibrocystic change of the breast presenting as a focal lesion mimicking breast cancer in MR imaging, J. Magn. Reson. Imaging 28 (6) (2008) 1499–1505.
[15] J.H. Chen, H. Liu, H.M. Baek, O. Nalcioglu, M.Y. Su, Magnetic resonance imaging features of fibrocystic change of the breast, Magn. Reson. Imaging 26 (9) (2008) 1207–1214.
[16] R.M. Mann, C.K. Kuhl, L. Moy, Contrast-enhanced MRI for breast cancer screening, J. Magn. Reson. Imaging (2019).
[17] C.K. Kuhl, S. Schrading, K. Strobel, H.H. Schild, R.D. Hilgers, H.B. Bieling, Abbreviated breast magnetic resonance imaging (MRI): first postcontrast subtracted images and maximum-intensity projection-a novel approach to breast cancer screening with MRI, J. Clin. Oncol. 32 (22) (2014) 2304–2310.
[18] G. Oldrini, B. Fedida, J. Poujol, J. Felblinger, I. Trop, P. Henrot, E. Darai, I. Thomassin-Naggara, Abbreviated breast magnetic resonance protocol: value of high-resolution temporal dynamic sequence to improve lesion characterization, Eur. J. Radiol. 95 (2017) 177–185.
[19] J.C.M. van Zelst, S. Vreemann, H.J. Witt, A. Gubern-Merida, M.D. Dorrius, K. Duvivier, S. Lardenoije-Broker, M.B.I. Lobbes, C. Loo, W. Veldhuis, J. Veltman, D. Drieling, N. Karssemeijer, R.M. Mann, Multireader study on the diagnostic accuracy of ultrafast breast magnetic resonance imaging for breast cancer screening, Invest. Radiol. (2018).
[20] M.U. Dalmiş, A. Gubern-Mérida, S. Vreemann, P. Bult, N. Karssemeijer, R. Mann, J. Teuwen, Artificial intelligence-based classification of breast lesions imaged with a multiparametric breast MRI protocol with ultrafast DCE-MRI, T2, and DWI, Invest. Radiol. (2019).
[21] N. Mori, Peritumoral apparent diffusion coefficients for prediction of lymphovascular invasion in clinically node-negative invasive breast cancer, Eur. Radiol. 26 (2) (2016) 331–339.
[22] R.L. Gutierrez, W.B. DeMartini, P.R. Eby, B.F. Kurland, S. Peacock, C.D. Lehman, BI-RADS lesion characteristics predict likelihood of malignancy in breast MRI for masses but not for nonmasslike enhancement, AJR Am. J. Roentgenol. 193 (4) (2009) 994–1000.